Fluidization and coating of very dense powders by fluidized bed chemical vapour deposition.

Philippe Rodriguez, Brigitte Caussat, Carine Ablitzer, Xavière Iltis, Méryl Brothier

Fluidization and coating of very dense powders by Fluidized Bed Chemical Vapour Deposition

Philippe Rodriguez[a], *Brigitte Caussat*[b,*], *Carine Ablitzer*[a], *Xavière Iltis*[a], *Méryl Brothier*[a]

[a] *CEA, DEN, DEC, SPUA, LCU, Cadarache, F-13108 Saint-Paul-lès-Durance, France*
[b] *Université de Toulouse, ENSIACET/INP Toulouse, LGC – UMR CNRS 5503 4 allée Émile Monso, BP 44362, 31030 Toulouse Cedex, France*

A B S T R A C T

The hydrodynamic behaviour of a very dense tungsten powder, 75 μm in median diameter and 19,300 kg/m^3 in grain density, has been studied in a fluidized bed at room temperature using nitrogen and argon as carrier gas. Even if fluidization was achieved, the small bed expansion indicated that it was imperfect. Then, the fluidization was studied at 400 °C in order to investigate the feasibility of coating this powder by Fluidized Bed Chemical Vapour Deposition (FBCVD). In particular, the influence of the H_0/D ratio (initial fixed bed height to reactor diameter) on the bed thermal behaviour was analyzed. It appeared that at least 1.5 kg of powder (corresponding to a H_0/D ratio of 1.8) was necessary to obtain an isothermal bed at 400 °C. Finally, first results about alumina coatings on the tungsten powder by FBCVD from aluminium acetylacetonate are detailed. They show that for the quite low temperatures tested, the coatings are uniform on all bed particles and are formed of amorphous carbon containing alumina. This study demonstrates the efficiency to combine fluidization (instead of spouted bed) and CVD to coat such very dense powders.

Keywords: CVD; Fluidization; Hydrodynamics; Dense powder; Alumina; Coating

1. Introduction

Fluidized bed technology has long been recognized as an efficient technique to perform gas–solid reaction and it has been employed in a wide range of industrial applications. Coupled with Chemical Vapour Deposition (CVD), gas–solid fluidization has a great potential to modify the surface properties of particles or to create new materials (Balaji et al., 2010; Vahlas et al., 2006). However, one constraint is that the powders to treat must be able to fluidize.

The available literature concerning the fluidization of very dense powders (i.e. whose grain density exceeds the upper limit of Geldart's classification, 10,000 kg/m^3) is scarce. Itagaki (1995) reported the fluidization of tungsten powder with a mean diameter ranging between 3 and 5 μm. WC–Co composite powders with 200 nm mean grain size were synthesized using high temperature fluidization technology (Gong and Ouyang, 2007). Nevertheless, these works concern relatively fine powders and we did not find reports concerning the fluidization of very dense particles with a mean diameter of several tens of microns. This fact is not really surprising because for particles with such characteristics, contact between gas and particles is generally achieved in spouted bed instead of fluidized bed (Geldart, 1973; Kunii and Levenspiel, 1991).

The present work deals with the hydrodynamic study of a tungsten powder in fluidized bed and its subsequent alumina coating by Fluidized Bed CVD. First, the fluidization of tungsten powder at room temperature and at 400 °C is discussed. Then, first results concerning the alumina coating of the tungsten powder by Fluidized Bed CVD are described.

2. Experimental

The fluidization tests of the tungsten powder at room temperature were carried out in a cylindrical column made of glass with an internal diameter of 0.05 m and a height of 1 m. An Inconel™ porous plate was used for the gas distribution.

* *Corresponding author*. Tel.: +33 5 34 32 36 32; fax: +33 5 34 32 36 97.
E-mail address: Brigitte.Caussat@ensiacet.fr (B. Caussat).

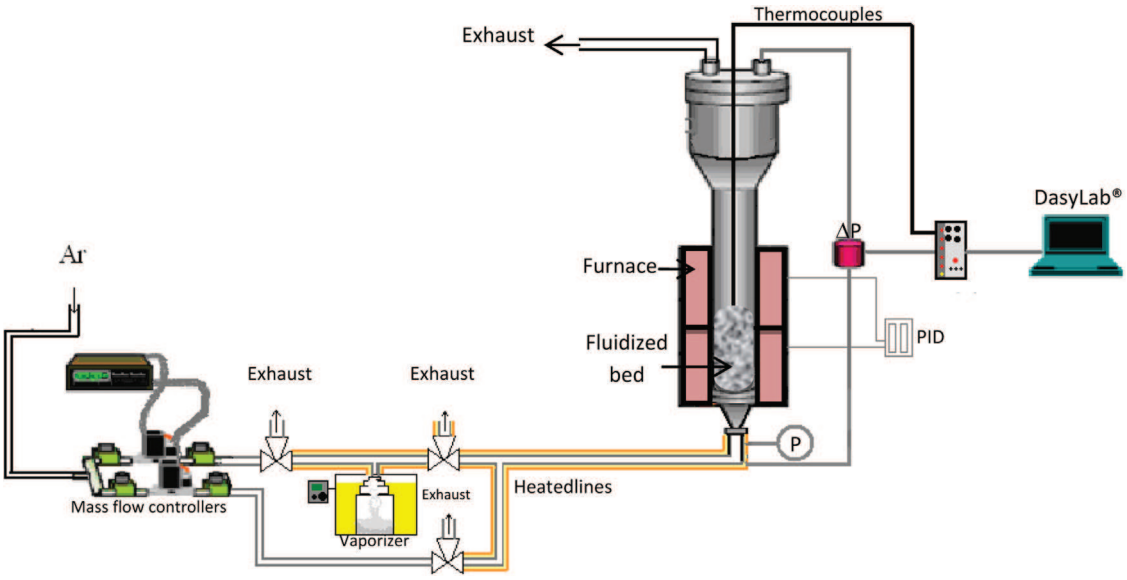

Fig. 1 – Schematic diagram of the FBCVD reactor.

Nitrogen carrier gas was supplied to the bottom of the bed through a mass flow controller. A differential fast response pressure sensor was used to measure the total pressure drop across the bed. A DasyLab® system enabled the on-line acquisition of the differential pressure.

The Fluidized Bed Chemical Vapour Deposition (FBCVD) reactor was made of a vertical cylindrical column of stainless steel and had the same dimensions as the glass column used for fluidization tests. Fig. 1 provides a schematic diagram of the reactor. The reactor was externally heated by a two-zone electrical furnace connected to a PID regulator and to two thermocouples fixed on the outer reactor walls. Several thermocouples were also bundled into a 6 mm diameter stainless steel tube and placed inside the reactor in order to monitor the bed temperatures at various heights. The same porous plate as in the glass column was used for the gas distribution and argon was used as carrier gas. The CVD precursor was evaporated from a stainless steel vaporizer placed in a thermostated bath and was fed into the reactor through heated lines to prevent condensation. The argon flow rates supplied directly to the bottom of the reactor and through the vaporizer were controlled by mass flow controllers. All CVD experiments were carried out at atmospheric pressure. A differential fast response pressure sensor with taps under the distributor and top of the column was used to measure the total pressure drop across the bed. Moreover for security reasons, an absolute pressure sensor allowed monitoring the total pressure below the distributor. As for the glass column setup, a DasyLab® system enabled the on-line acquisition of the differential pressure, the total pressure and the axial profile of bed temperatures. The FBCVD reactor was also used to perform tungsten powder fluidization tests at room temperature and at 400 °C using argon as carrier gas.

In this study, tungsten powder (T-1220) produced by CERAC, Inc. and supplied by NEYCO was used. According to the characteristics provided by the producer, the grain density is 19,300 kg/m^3. Scanning electron microscopy (SEM) observations highlighted that particles are non-spherical and faceted as shown in Fig. 2a. The particle size distribution (PSD) values measured by laser scattering (performed with a Beckman Coulter LS^{TM} 13 320 particle size analyser) indicated that the distribution of the particle diameters D_{10}/D_{90} is 50 μm/105 μm with a median diameter (D_{50}) of about 75 μm; the corresponding results are shown in Fig. 2b.

The alumina coatings were performed using aluminium acetylacetonate $Al(C_5O_2H_7)_3$ (99%) as a single-source MetalOrganic (MO) precursor. It was purchased from Strem Chemicals, Inc., under the form of a fine grey powder.

The fluidization hydrodynamics was studied by plotting the bed pressure drop and expansion versus increasing and decreasing gas superficial velocities. A normalized bed

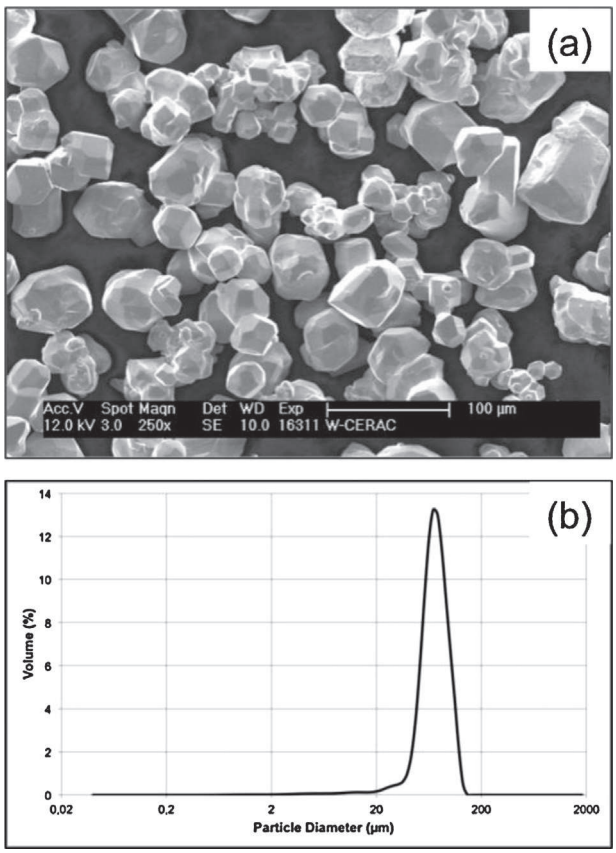

Fig. 2 – Characterization of the tungsten powder used in this study: (a) SEM micrograph and (b) particle size distribution (PSD).

pressure drop ΔP^* was calculated by dividing the experimental bed pressure drop by the theoretical bed pressure drop (equal to the bed weight per column cross-sectional area). A normalized bed expansion H^* was also measured as the ratio between the average expanded bed height and the fixed bed height. These heights were measured using a rule fixed on the glass column walls, with uncertainties lower than 10%.

The morphology and the composition of the initial powder and of the coated particles were observed by scanning electron microscopy coupled with EDS analyses (Philips XL 30 FEG and LEO 435 VP).

3. Fluidization study of tungsten powder

The hydrodynamic study of the tungsten powder had two main objectives. First, the ability to fluidize of this powder was not obvious. Indeed, due to its very high density, this powder cannot be positioned into the Geldart's classification (Geldart, 1973). However, it is well-known that contact between gas and Geldart's group D particles, i.e. either large or dense particles, is generally achieved in spouted bed instead of fluidized bed (Kunii and Levenspiel, 1991). Second, and after validation of the first point, we had to determine the necessary experimental conditions to obtain a fluidized bed with a temperature stabilized at least at 400 °C which was the lower temperature limit to obtain an efficient decomposition of our single-source CVD precursor. For this point, we carefully studied the influence of the H_0/D ratio (initial fixed bed height to reactor inner diameter) on the bed thermal behaviour. Our aim was to obtain bed temperatures as isothermal as possible since temperature is a key parameter to obtain uniform coatings by CVD.

An example of the fluidization results obtained at room temperature using 1.3 kg of powder is illustrated in Fig. 3.

The experimental plots obtained for normalized bed pressure drop versus decreasing gas velocity (Fig. 3a), coupled with observations of the hydrodynamics of the bed through the glass column, prove that fluidization was reached (Kunii and Levenspiel, 1991). Using nitrogen as carrier gas, the measured minimum fluidization velocity (U_{mf}) is close to 4.2 cm/s. Even if fluidization was reached, this latter remained difficult as indicated by the hysteresis observed between experimental points obtained for normalized bed pressure drop versus increasing and decreasing gas velocities (Weber and Hrenya, 2007). The fact that fluidization is imperfect was confirmed by the very low bed expansion observed, i.e. only 10% for a fully fluidized bed, as illustrated in Fig. 3b. This is probably due to the very high value of powder density and to a lesser extent, to the fact that particles are not spherical (Kunii and Levenspiel, 1991).

As shown in Fig. 3a, for the tests performed in the glass column with nitrogen as carrier gas, ΔP^* has never reached exactly the theoretical bed pressure drop plateau. This phenomenon could be explained by the fact that a low percentage of tungsten particles were deposited onto the glass column walls and, due to the very high density of tungsten particles, this could have significantly changed the bed weight and the corresponding theoretical bed pressure drop. Moreover, when experiments were carried out with 1.3 kg or more of tungsten powder, the bed pressure drops were closed to the differential fast response pressure sensor upper limit. This technological limitation could have increased the experimental measurement errors for the highest gas velocities. It is worth noting that for all the experiments carried out in the stainless steel reactor with argon as carrier gas and without experimental limitation concerning the differential pressure sensor, a fluidization plateau close to the theoretical value was observed.

Table 1 – Comparison between experimental minimum fluidization velocities in N_2 and Ar and calculated ones from two classical correlations.

Fluidization gas	Nitrogen	Argon
Experimental U_{mf} (cm/s)	4.2	3
U_{mf} from Bourgeois and Grenier correlation (cm/s)	4.5	3.6
U_{mf} from Thonglimp correlation (cm/s)	4	3.2

Using argon as carrier gas, the measured minimum fluidization velocity is close to 3 cm/s. Table 1 compares the experimental U_{mf} in N_2 and Ar with those obtained using two classical correlations, that of Bourgeois and Grenier (1968) and that of Thonglimp et al. (1984), based on Reynolds and Archimede dimensionless groups. The calculated values are very close to the experimental ones, showing the good accuracy of the experimental measurements. When analysing the influence of the gas physical properties on the various parts of the correlations, it clearly appears that the U_{mf} value in Ar is lower than that in N_2 because of the higher viscosity of argon.

Once we have demonstrated that it was possible to fluidize this tungsten powder, the second step of the hydrodynamic study was to determine the optimal experimental conditions to obtain a fluidized bed with a temperature stabilized at least at 400 °C. For our application, low bed weights are required. Then, the aim of this experimental part was to obtain an isothermal and fully fluidized bed of particles with the lowest possible bed weight. Thermal profiles were recorded for various bed weights. Table 2 details the correspondence between bed weights, bed heights and H_0/D ratios and also provides the imposed wall temperatures, the resulting bed thermal gradient and bed temperature at 2.5 cm above the distributor after 2 h 30 of heating. Experiments were carried out in the FBCVD reactor using preheated argon at 120 °C as carrier gas.

Analyses of thermal profiles showed that for the lowest bed heights studied (i.e. $H_0/D < 1$), the target bed temperature (400 °C) could not be reached. Even after 2 h 30 of heating process and furnace set point fixed at 800 °C, the bed temperature stagnated at about 330 °C. Only H_0/D ratios higher than or equal to 1 allowed reaching a bed temperature around 400 °C. However, for H_0/D ratios of 1, the furnace set point had to be fixed at 850 °C and the bed was not isothermal. Indeed, thermal gradients ΔT between the bottom and the top of the bed reached 50 °C which is unacceptable for subsequent CVD coating. It is well known that higher the H_0/D ratio is, better the thermal and mass transfers are, and that H_0/D ratios up to 4–5 are generally used for FBCVD coatings (Vahlas et al., 2006). Such values were obviously impossible to carry out because a H_0/D ratio of 4 corresponds to a bed weight as high as 3.4 kg, which was not conceivable for preliminary tests and for our further application. So, a compromise had to be found between an acceptable thermal behaviour and a reasonable bed weight. For bed weights of 1.5 kg corresponding to H_0/D ratios of 1.8, a satisfactory thermal profile was obtained with a bed temperature stabilized around 400 °C after 2 h of heating process and furnace set point fixed at 750 °C. The ratio between the gas velocity at 400 °C and the minimum fluidization velocity (U_g/U_{mf}) was fixed at approximately 3.5. For such experimental parameters, the bed was isothermal: ΔT between the bottom and the top of the bed was less than 2 °C.

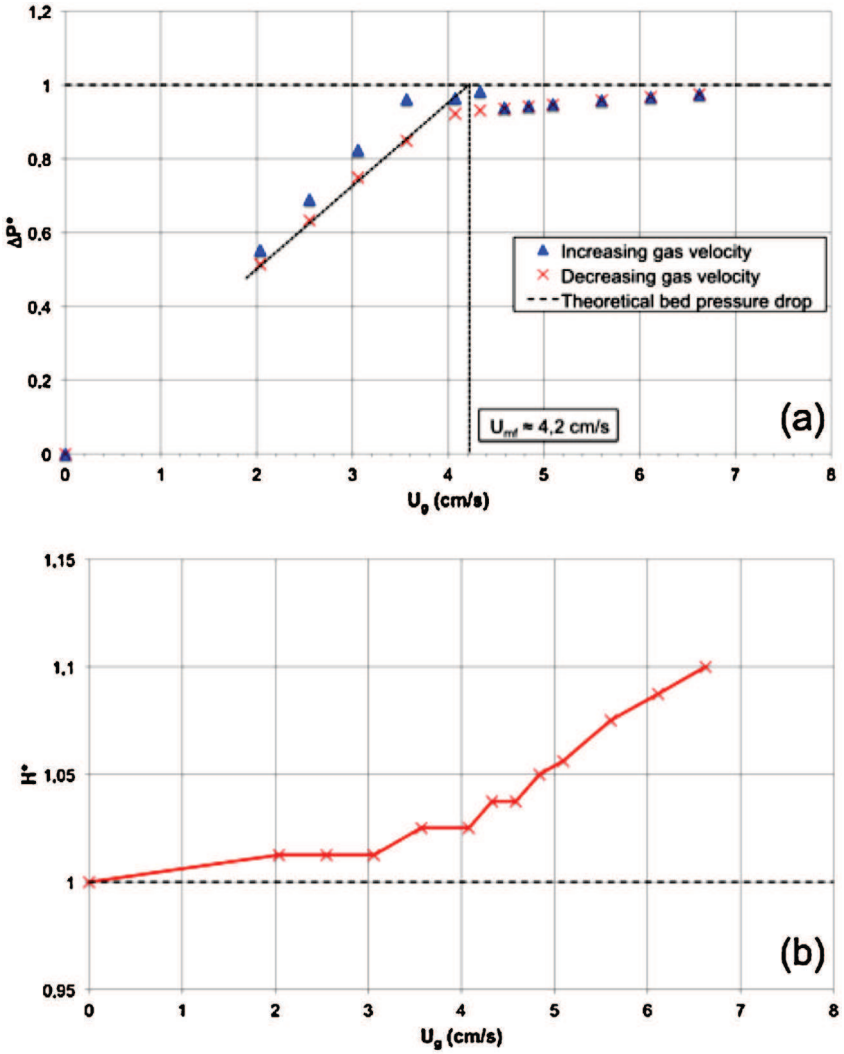

Fig. 3 – Normalized (a) pressure drop and (b) expansion versus decreasing nitrogen superficial velocities for a bed of tungsten powder.

The important gap between the reactor walls and the bed temperatures could be explained by the very low bed expansions measured, as shown in Fig. 3b: only 10% of expansion for a fully fluidized bed of tungsten particles whereas standard values obtained for more conventional powders generally range between 30 and 40% (Kunii and Levenspiel, 1991). These very low values imply low thermal transfers between particles and reactor walls. We have verified that these bed expansions follow the correlation of Richardson and Zaki (1954) for Reynolds numbers lower than 0.3. This good agreement shows the good accuracy of measurements and indicates that these low values are due to the density of the powder.

4. FBCVD of alumina on tungsten powder

Using the experimental parameters described in the previous section in particular 1.5 kg of powder for each run, we successfully performed the FBCVD of alumina on several sets of tungsten powder by varying bed temperature, carrier gas flow rate sent through the vaporizer line and coating duration. All the results detailed below are representative of the whole results obtained.

Fig. 4 shows a typical thermal profile obtained during CVD experiments. The heating process was organized in two steps of 1 h, in order to progressively increase the powder

Table 2 – Bed weights, bed heights, H_0/D ratios, imposed wall temperatures, measured bed thermal gradients and bed temperatures at 2.5 cm above the distributor after 2 h 30 of heating.

Bed weight (kg)	Bed height (cm)	H_0/D ratio	Wall temperature (°C)	Bed thermal gradient (°C)	Bed temperature 2.5 cm above the distributor (°C)
0.4	2.4	0.48	800	>50	350
0.6	3.6	0.72	800	>50	350
0.85	5.1	1.01	850	50	410
1	5.9	1.19	850	20	410
1.5	8.9	1.78	750	<2	420
1.7	10.1	2.02	700	<2	420

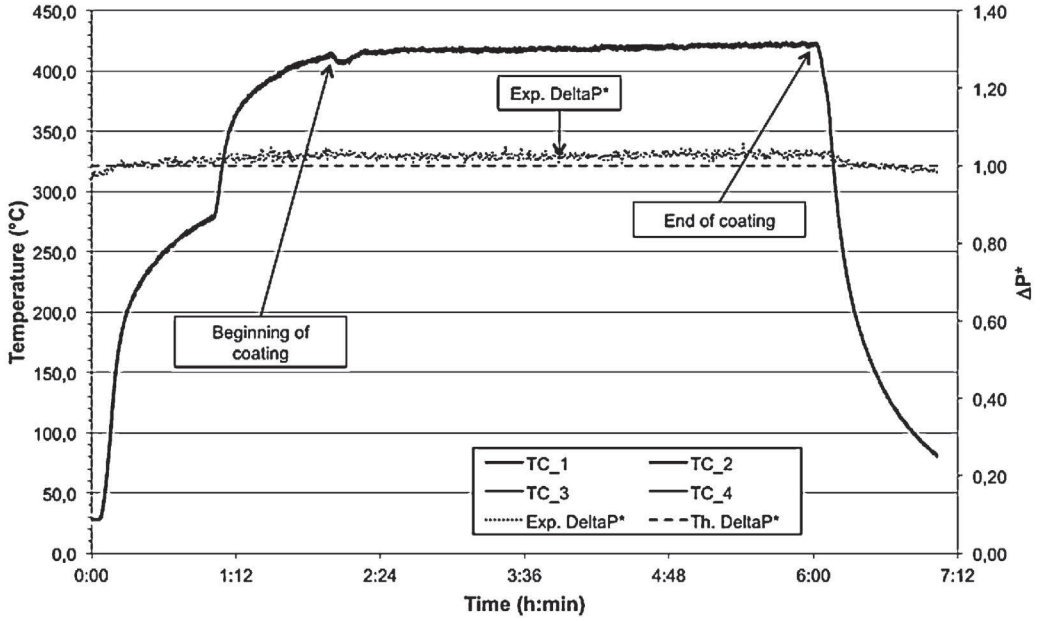

Fig. 4 – Typical bed thermal profile and theoretical bed pressure drop obtained during FBCVD of alumina on tungsten powder (heights above the distributor for thermocouple TC_1: 1 cm, TC_2: 2.5 cm, TC_3: 5 cm, TC_4: 7 cm).

temperature without over heating the reactor walls. The isothermal behaviour of the bed appears in Fig. 4, since the four thermocouples placed inside the particle bed at different heights indicated the same temperature values. Once the desired coating temperature was reached, the coating procedure began. We noticed a slight decrease of the bed temperature during the first minutes of coating. This may be related to the precursor decomposition that requires energy supply. At the beginning of the coating, the necessary energy is provided by the fluidized bed, leading to a slight decrease of its temperature. Then, after a few minutes of heating regulation, the bed temperature is stabilized.

As illustrated in Fig. 4, the experimental normalized bed pressure drop (called *Exp. DeltaP**) was calculated and compared with the theoretical normalized bed pressure drop (called *Th. DeltaP**) during all experiments. The obtained results clearly indicate that the tungsten particle bed remained fully fluidized during all runs.

After experiments, the difference between coated and uncoated particles is obvious to the naked eye. Whereas uncoated particles are metallic grey, the coated particles exhibited a brown tint. This colour could be surprising for alumina coatings. However, several works, in which alumina coatings were obtained from aluminium acetylacetonate precursor in our range of temperature, i.e. 390–450 °C, have reported that obtained films exhibited orange-claret (Minkina, 1993), golden brown (Nable et al., 2003) or tan and dark tan (Nguyen et al., 2002) tints. These colours could be explained by an alumina film contamination due to carbon and pyrolysis by-products incorporation. The chemical reactions leading to alumina deposition from aluminium acetyl acetonate are complex and poorly known (Minkina, 1993; Devi et al., 2002; Singh and Shivashankar, 2002; Pflitsch et al., 2007). Under argon, some simplified reactions have been proposed (Rhoten and Devore, 1997), considering that $Al(acac)_3$ first decomposes in the gas phase:

$$Al(C_5H_7O_2)_3 \rightarrow Al(C_5H_7O_2)_2OH + C_5H_6O \quad (R1)$$

Then, the gaseous intermediate can react on surface to form alumina:

$$2Al(C_5H_7O_2)_2OH \rightarrow Al_2O_3 + 2C_5H_8O_2 + 2C_5H_6O + H_2O \quad (R2)$$

Some studies have shown that carbon incorporation is favoured at low temperature due to an incomplete decomposition of the reactive species into Al_2O_3 on the substrate surface (Devi et al., 2002; Pflitsch et al., 2007).

Moreover, at these relative low temperatures, aluminium oxide films obtained by MOCVD (i.e. CVD from a Metal Organic precursor) are mainly amorphous (Nable et al., 2003a). The uniform tint of particles after deposition indicates that all particles were uniformly treated. This has been confirmed by SEM, as detailed below.

The deposited mass was so low that it was not possible to measure it by bed weighing before and after deposition. As a consequence, the deposition yield, the ratio between the masses of deposited Al and of sublimated Al, is very low. This is probably due to the low bed temperature tested, leading to weak precursor decomposition.

In order to study the differences between coated and uncoated particles at microscopic scale, all the samples have been observed by SEM coupled with EDS analyses. The surface morphology of uncoated tungsten particles is relatively smooth as shown in Fig. 5a. Moreover, EDS analyses performed on uncoated samples show the different characteristic peaks of tungsten and, for some particles, the peak of oxygen. This latter is probably due to a partial oxidation of tungsten powder during handling under air.

The SEM analyses of coated particles (Fig. 5b) exhibit pronounced morphologic differences: the surface roughness is clearly increased and the presence of a coating film is obvious. Even if Al K_α peak is partially overlapped by W M_α peak and that alumina films are very thin (probably less than 100 nm according to calculated film thicknesses from mass balances), EDS analyses on coated samples show oxygen, carbon and aluminium peaks. Tungsten was also detected because EDS analyses concern thicknesses higher than those of alumina deposits. The relative comparison of the EDS

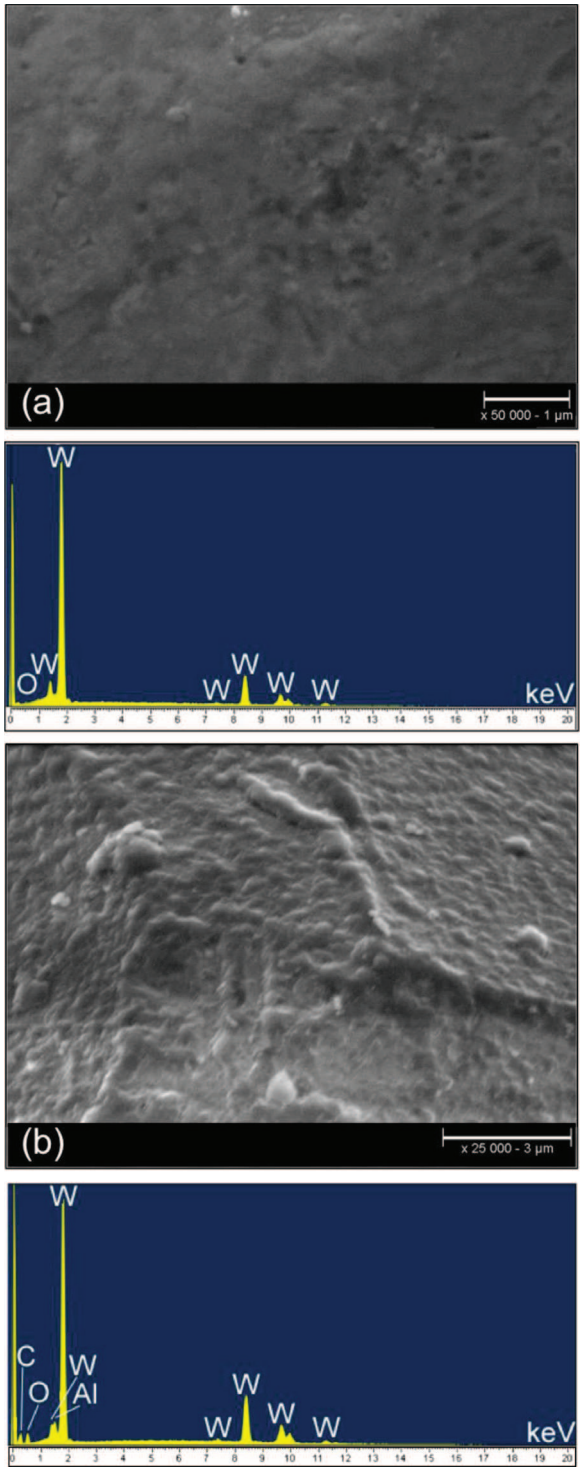

Fig. 5 – SEM micrographs and corresponding EDS analyses of (a) uncoated and (b) alumina coated tungsten powder.

spectra of uncoated and coated particles indicates that, on these latter, an alumina film with carbon impurities was obtained. This result is in good accordance with previous works reported in literature, as already mentioned (Minkina, 1993; Nable et al., 2003).

The average layer thickness was measured from SEM observations of crushed coated powder using a backscattered electron (BSE) detector. A characteristic example of results is given in Fig. 6. The film thickness appears to be lower than 100 nm and uniform on the particle surface and from one particle to another. Some ICP-AES measurements have been attempted, but due to this very low thickness, they did not

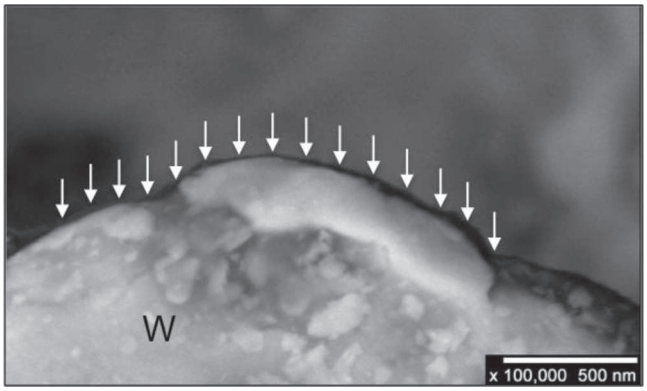

Fig. 6 – SEM observations of crushed coated powder using a backscattered electron (BSE) detector (the arrows show the deposited film).

provide any quantitative result about the film composition, except the fact that aluminium is well deposited on the powder surface.

5. Conclusion

The fluidization of a very dense powder (i.e. whose grain density exceeds the upper limit of Geldart's classification, 10,000 kg/m^3) was successfully demonstrated, which could not be predicted from Geldart's diagram. This work was performed using tungsten particles of 75 μm in median diameter and 19,300 kg/m^3 in grain density.

The experimental minimum fluidization velocities and bed expansions in nitrogen and argon were determined and compared with theoretical correlations. The results showed that, even if fluidization is achieved, the bed expansion is very low due the powder high density, involving low thermal transfers between powder and reactor walls. However, the analysis of axial thermal profiles for different bed weights allowed finding experimental parameters insuring isothermal conditions compatible with Fluidized Bed Chemical Vapour Deposition of alumina at 400 °C.

First characterizations of samples after CVD suggest that alumina films formed from aluminium acetylacetonate $Al(C_5O_2H_7)_3$ as single source precursor are probably amorphous and carbon contaminated. In spite of the low bed expansion, all particles appear to be uniformly coated. The deposit thickness is lower than 100 nm, certainly due to the low temperature tested involving weak precursor decomposition. As far as we know, this study is probably the first one to demonstrate the efficiency to combine fluidization (instead of spouted bed) and CVD to coat such very dense powders of several tens of microns in diameter. Additional experiments are planned to test higher deposition temperatures in order to limit carbon contamination.

Acknowledgements

The authors would like to thank Michel Molinier, Etienne Prevot, Marie Line De Solan from LGC and Hélène Rouquette from CEA for their technical support.

References

Balaji, S., Du, J., White, C.M., Ydstie, B.E., 2010. Multi-scale modeling and control of fluidized beds for the production of solar grade silicon. Powder Technol. 199, 23–31.
Bourgeois, P., Grenier, P., 1968. The ratio of terminal velocity to minimum fluidization velocity for spherical particles. Can. J. Chem. Eng. 46, 325–331.
Devi, A., Shivashankar, S.A., Samuelson, A.G., 2002. MOCVD of aluminium oxide films using aluminium β-diketonates as precursors. J. Phys. IV 12, 139–146.
Geldart, D., 1973. Types of gas fluidization. Powder Technol. 7, 285–292.
Gong, N., Ouyang, Y., 2007. The study of synchronous reduction-carbonization of V_2O_3,Cr_2O_3 and W–Co composite oxides in fluidization. Mater. Sci. Forum 534/536, 1245–1248.
Itagaki, T., 1995. Coating of HfC on tungsten powder by fluidized bed CVD. J. Jpn. Inst. Met. 59, 1157–1164.
Kunii, D., Levenspiel, O., 1991. Fluidization Engineering, 2nd ed. Butterworth-Heinemann Ltd., Newton, MA, USA.
Minkina, V.G., 1993. Study of the pyrolysis kinetics of aluminum acetylacetonate in the gaseous-phase. Inorg. Mater. 29, 1400–1401.
Nable, J.C., Gulbinska, M.K., Kmetz, M.A., Suib, S.L., Galasso, F.S., 2003. Aluminum oxide and chromium oxide coatings on ceramic fibers via MOCVD. Chem. Mater. 15, 4823–4829.
Nable, J., Gulbinska, M., Suib, S.L., Galasso, F., 2003a. Aluminum oxide coating on nickel substrate by metal organic chemical vapor deposition. Surf. Coat. Technol. 173, 74–80.
Nguyen, Q.T., Kidder Jr., J.N., Ehrman, S.H., 2002. Hybrid gas-to-particle conversion and chemical vapor deposition for the production of porous alumina films. Thin Solid Films 410, 42–52.
Pflitsch, C., Viefhaus, D., Bergmann, U., Atakan, B., 2007. Organometallic vapour deposition of crystalline aluminium oxide films on stainless steel substrates. Thin Solid Films 515, 3653–3660.
Richardson, J.F., Zaki, W.N., 1954. Sedimentation and fluidization: part I. Trans. Inst. Chem. Eng. 32, 35–53.
Rhoten, M.C., Devore, T.C., 1997. Evolved gas phase analysis investigation in the reaction between Tris(2,4-pentanedionato)aluminium and water vapour in Chemical Vapor Deposition processes to produce alumina. Chem. Mater. 9, 1757–1764.
Singh, M.P., Shivashankar, S.A., 2002. Low pressure MOCVD of Al_2O_3 films using aluminium acetylacetonate as precursor: nucleation and growth. Surf. Coat. Technol. 161, 135–143.
Thonglimp, V., Hiquily, N., Laguérie, C., 1984. Minimum velocity of fluidization and expansion of gas fluidized beds. Powder Technol. 38, 233–253.
Vahlas, C., Caussat, B., Serp, Ph., Angelopoulos, G., 2006. Principles and applications of CVD powder technology. Mater. Sci. Eng. Res. 53 (1–2), 1–72.
Weber, M.W., Hrenya, C.M., 2007. Computational study of pressure-drop hysteresis in fluidized beds. Powder Technol. 177, 170–184.